Environmental Research 181 (2020) 108905

Contents lists available at ScienceDirect

Environmental Research

journal homepage: www.elsevier.com/locate/envres

Recirculation ratio regulates denitrifying sulfide removal and elemental sulfur recovery by altering sludge characteristics and microbial community composition in an EGSB reactor

Fan Chen[a], Zhi-Ling Li[a,*], Miao Lv[a], Cong Huang[a], Bin Liang[b], Ye Yuan[b,c], Xiao-Qiu Lin[a], Xiang-Yu Gao[a], Ai-Jie Wang[a,b,**]

[a] State Key Laboratory of Urban Water Resources and Environment, School of Environment, Harbin Institute of Technology, Harbin, 150090, China
[b] Key Laboratory of Environmental Biotechnology, Research Center for Eco-Environmental Sciences, Chinese Academy of Sciences, Beijing, 100085, China
[c] School of Environmental Science and Engineering, Yancheng Institute of Technology, Yancheng, 224051, China

ARTICLE INFO

Keywords:
Denitrifying sulfide removal
Expanded granular sludge blanket (EGSB)
Recirculation ratio
Elemental sulfur recovery
Microbial community composition

ABSTRACT

Expanded granular sludge blanket (EGSB) is regarded as a promising reactor to carry out denitrifying sulfide removal (DSR) and elemental sulfur (S^0) recovery. Although the recirculation ratio is an essential parameter for EGSB reactors, how it impacts the DSR process remains poorly understood. Here, three lab-scale DSR-EGSB reactors were established with the different recirculation ratios (3:1, 6:1 and 9:1) to evaluate the corresponding variations in pollutant removal, S^0 recovery, anaerobic granular sludge (AGS) characteristics and microbial community composition. It was found that an intermediate recirculation ratio (6:1) could facilitate long-term reactor stability. Adequate recirculation ratio could enhance S^0 recovery, but an excessive recirculation ratio (9:1) was likely to cause AGS fragmentation and biomass loss. The S^0 desorbed more from sludge at higher recirculation ratios, probably due to the enhanced hydraulic disturbance caused by the increased recirculation ratios. At the low recirculation ratio (3:1), S^0 accumulation as inorganic suspended solids in AGS led to a decrease in VSS/TSS ratio and mass transfer efficiency. Although typical denitrifying and sulfide-oxidizing bacteria (e.g., *Azoarcus*, *Thauera* and *Arcobacter*) were predominant in all conditions, facultative and heterotrophic functional bacteria (e.g., *Azoarcus* and *Thauera*) were more adaptable to higher recirculation ratios than autotrophs (e.g., *Arcobacter*, *Thiobacillus* and *Vulcanibacillus*), which was conducive to the formation of bacterial aggregates to response to the increased recirculation ratio. The study revealed recirculation ratio regulation significantly impacted the DSR-EGSB reactor performance by altering AGS characteristics and microbial community composition, which provides a novel strategy to improve DSR performance and S^0 recovery.

1. Introduction

A large amount of sulfate and ammonium/nitrate-laden wastewater is generated from pulp production, pharmaceutical and refinery industries (Show et al., 2013). Sulfide (H_2S, HS^- and S^{2-}), a toxic, odorous and corrosive metabolite, is commonly yielded during anaerobic sulfate reduction (Hao et al., 2014). Nitrate (NO_3^-) is another metabolite produced from biological ammonium nitrification processes (Yuan et al., 2019). Therefore, sulfide and nitrate often coexist in industrial wastewater treatment plants (Wu et al., 2016). Recently, the denitrifying sulfide removal (DSR) process aiming at the simultaneous removal of nitrogen and carbon and recovery of elemental sulfur (S^0) has been developed (Huang et al., 2015a, 2018). In the DSR process, sulfide oxidizing bacteria (SOB) can utilize NO_3^- as an electron acceptor to transfer sulfide to elemental sulfur (S^0) (Cui et al., 2019; Huang et al., 2019), and meanwhile, NO_3^- can be reduced to nitrogen gas (N_2) by autotrophic and/or heterotrophic denitrifiers (Zhang et al., 2018).

Several bioreactor systems including stirred tank reactor (CSTR), anaerobic baffled reactor (ABR), up-flow anaerobic sludge bioreactor (UASB), expanded granular sludge blanket (EGSB) reactor have been used to conduct DSR process (Chen et al., 2017; Huang et al., 2015a, 2015b; Zhang et al., 2018). Among them, EGSB reactor is designed with a high height/diameter ratio and operated at high up-flow velocities

* Corresponding author.
** Corresponding author. State Key Laboratory of Urban Water Resources and Environment, School of Environment, Harbin Institute of Technology, Harbin, 150090, China
E-mail addresses: lzlhit@163.com (Z.-L. Li), waj0578@hit.edu.cn (A.-J. Wang).

https://doi.org/10.1016/j.envres.2019.108905
Received 22 September 2019; Received in revised form 7 November 2019; Accepted 7 November 2019
Available online 09 November 2019
0013-9351/

(Faria et al., 2019). The increased flow velocity can be obtained by applying high recirculation ratios, which is defined as the ratio of the returned flow rate of EGSB effluent to the inlet flow rate of EGSB influent. EGSB reactor is regarded as an effective and promising reactor configuration for DSR process due to the improved substrate-biomass contact favored by high hydraulic mixing intensification (Chen et al., 2009; Wang et al., 2009). Therefore, several DSR-EGSB systems have been developed to study the performance, microbial community structure and function in response to the different hydraulic retention time (HRT), sulfide/nitrate/COD loading ratios and trophic conditions (Chen et al., 2008, 2009; Huang et al., 2016, 2017; Zhang et al., 2018).

For DSR-EGSB systems, the recirculation ratio is an important parameter affecting hydrodynamic conditions and mass transfer efficiencies of the biochemical reactions (Bhattacharyya and Singh, 2010; Zheng et al., 2012). On the other hand, dilution of the influent by applying effluent internal circulation can alleviate toxicity inhibition of sulfides on microorganisms (Jin et al., 2013). To date, although high-efficiency S^0 generation has been achieved by applying DSR-EGSB systems, part of the generated S^0 adheres to the surface or inside of anaerobic granular sludge (AGS), which hinders the S^0 further recovery from effluent (Chen et al., 2016; Di Capua et al., 2019; Huang et al., 2018). The considerable S^0 accumulation in AGS tends to cause bioreactor clogging and a decline in mass transfer efficiency, which may be one of the major obstacles in the long-term operation of DSR-EGSB systems. In addition, if the generated S^0 cannot be timely separated from AGS, it will be further oxidized or reduced due to the presence of bacteria in AGS (Huang et al., 2018). It is worth mentioning that S^0 distribution between AGS and effluent may be optimized by the regulation of hydraulic flushing conditions, which can be achieved by changing recirculation ratios. However, as far, how recirculation ratio influences the S^0 distribution and recovery under DSR process is largely unknown. Facing the hydraulic conditions at different recirculation ratios, the AGS characteristics, as well as the microbial community structure and function, may be gradually influenced. Additionally, how recirculation ratio regulates the DSR-EGSB performance by influencing AGS characteristics and the functional community structure remains poorly understood.

Therefore, in this study, three lab-scale DSR-EGSB systems were established with different recirculation ratios (3:1, 6:1 and 9:1) to evaluate the effect of recirculation ratio on C/N/S removal, S^0 recovery, AGS characteristics and microbial community structure. Objectives of the study were to reveal (i) whether recirculation ratio regulation could facilitate the stability and performance of DSR-EGSB systems, including C/N/S removal and S^0 distribution and recovery, and (ii) how recirculation ratio influenced the AGS characteristics and microbial community structure and further regulated DSR-EGSB performance.

2. Materials and methods

2.1. Reactor set-up, inoculum and influent condition

Three identical lab-scale EGSB reactors were continuously operated at the fixed recirculation ratios of 3:1 (R1), 6:1 (R2) and 9:1 (R3), respectively. The reactor was made of plexiglass and had an effective volume of 2.2 L (60 mm in diameter and 912 mm in height). The detailed setup of the DSR-EGSB system was shown in Fig. S1. Each reactor was inoculated with 1 L of anaerobic sludge taken from previous UASB reactors for the DSR process (Huang et al., 2017). The volatile suspended solids (VSS) and suspended solids (SS) of the seed sludge were 20.99 g/L and 41.50 g/L, respectively. As shown in Table S1, the influent was consisting of sulfide-S (200 mg/L), NO_3^--N (105 mg/L) and acetate (Ac^-) –C (113 mg/L), to achieve the desired sulfide-S/nitrate-N mol ratio of 5/6 and acetate-C/nitrate-N mol ratio of 1.26/1 (Huang et al., 2015a). The essential trace elements were also added as described previously (Huang et al., 2018). The influent pH was maintained at 8.0 ± 0.4 by adding sodium bicarbonate (1.5 g/L). The synthetic wastewater with inorganic and organic carbon sources was used to form a mixotrophic condition. Oxygen-free deionized water was used to synthesis wastewater. The synthetic wastewater influent connected with the nitrogen bag was continuously supplied from a sealed storage tank. In acclimation stage, hydraulic retention time (HRT) was fixed at 12 h. After acclimation for 7 d, DSR-EGSB reactors were continuously operated for 82 d at a reduced HRT of 4 h. The recirculation ratios were controlled by applying peristaltic pumps. All reactors were operated at an ambient temperature of 25 ± 3 °C.

2.2. Chemicals, analytical methods and calculations

Sodium sulfide nonahydrate ($Na_2S{\cdot}9H_2O$; ≥98% purity), potassium nitrate (KNO_3; ≥99% purity) and sodium acetate anhydrous (CH_3COONa; ≥99% purity) were purchased from Sigma-Aldrich (St. Louis, MO, USA). All other chemicals used to prepare trace element solutions or analytical standards were of analytical reagent grade and purchased from Sinopharm Chemical Reagent Co. Ltd (Shanghai, China). Influent and effluent samples (5 mL) were collected from the inlet and outlet of the reactor daily and analyzed immediately. Sulfide concentration, including H_2S, HS^- and S^{2-} in liquid were determined by submethyl blue spectrophotometric method according to GB/T 16489-1996 (China). Liquor pH was measured by pH meter (pHS-25, Shanghai, China). All samples were centrifuged at 12,000 rpm for 10 min and then filtered through a 0.22 mm Millipore filter for subsequent anion analysis. The concentrations of sulfate (SO_4^{2-}), sulfite (SO_3^{2-}), thiosulfate ($S_2O_3^{2-}$), nitrate (NO_3^-), nitrite (NO_2^-) and acetate (CH_3COO^-) were measured by anion chromatograph (ICS-3000A; Dionex, USA) with a column (IonPac AG4AAS4A-SC 4 mm, Dionex, USA).

The concentration of total produced S^0 (mg/L) both in sludge and effluent was calculated according to the following equation (De Graaff et al., 2012): $[S^0]_t = [H_2S + HS^- + S^{2-}]_{in} + [SO_4^{2-}]_{in} + [S_2O_3^{2-}]_{in} - [H_2S + HS^- + S^{2-}]_{eff} - [SO_4^{2-}]_{eff} - [S_2O_3^{2-}]_{eff}$. As a highly reactive S-species intermediate, SO_3^{2-} was negligible during sulfide-driven autotrophic denitrification. The S^0 transformation ratio was calculated as: S^0 transformation ratio (%) = $[S^0]_t/([H_2S + HS^- + S^{2-}]_{in} - [H_2S + HS^- + S^{2-}]_{eff}) \times 100\%$. The S^0 in the effluent ($[S^0]_{eff}$) (mg/L) was analyzed using an HPLC (Agilent 1200, Agilent Technologies, CA, USA) equipped with a Li-Chrospher 100 RP 18 column (Merck Chromolith, Darmstadt, Germany) and a UV detector at 263 nm (Huang et al., 2018). The S^0 recovery ratio was the ratio of S^0 in the effluent ($[S^0]_{eff}$) to total produced S^0 ($[S^0]_t$) and calculated as $R_{S0} = [S^0]_{eff}/[S^0]_t \times 100\%$. The p-value determined by one-way analysis of variance (one-way ANOVA) was used to test for differences among R1, R2 and R3. The S^0 transformation ratio, NO_3^- removal ratio and Ac^- removal ratio were used as numerical response data for one-way ANOVA, respectively. Granule sludge size distribution by weight was measured by sieving method (Ji et al., 2009). Briefly, at the end of the operation, 20 mL AGS was sampled and passed through standard sieves (2.0 mm, 1.0 mm, 0.6 mm and 0.3 mm) with water as the rinsing medium. AGS with the different particle sizes was dried to measure total suspended solids (TSS) and calculated its proportion in total AGS dry weight. TSS and volatile suspended solids (VSS) were determined according to the gravimetric method (He et al., 2019).

2.3. DNA extraction and 16S rRNA gene sequencing

After 82 d of continuous operation, the fresh mixture (10 mL) of granular biomass and suspension biomass was collected from the sampling ports of the three EGSB bioreactors and immediately stored at −80 °C for DNA extraction. The PowerSoil DNA Isolation kit (MoBio Laboratories Inc, USA) was used for DNA extraction according to the manufacturer's instructions. The concentration and purity of the extracted DNA were examined by a Nanophotometer (P-class, Implen, Germany). DNA samples were sent for PCR amplification focusing on

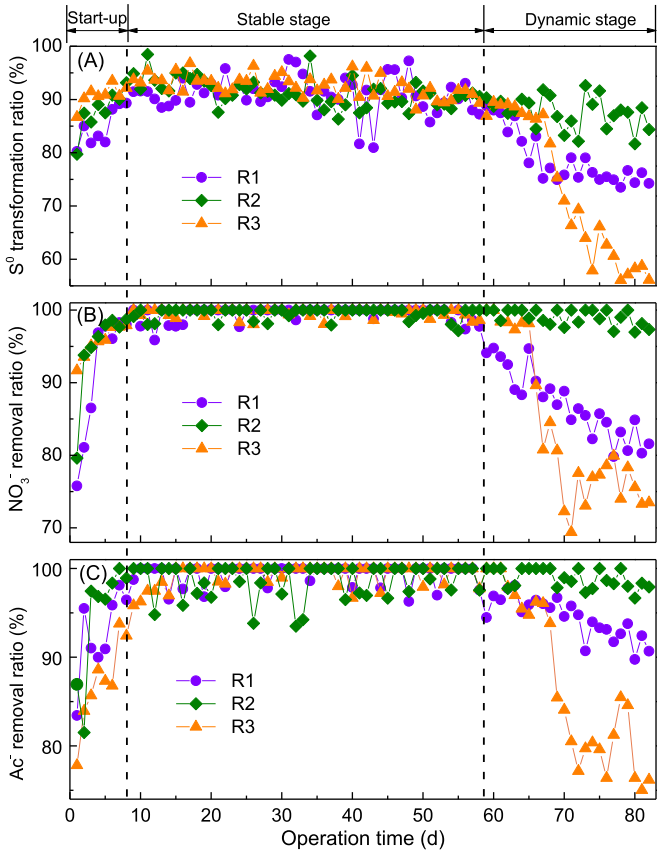

Fig. 1. Performance of the DSR-EGSB reactor at a recirculation ratio of 3:1 (R1), 6:1 (R2) and 9:1 (R3), respectively. (A) S^0 transformation ratio; (B) NO_3^- removal ratio; (C) Ac^- removal ratio.

bacterial V1 to V3 region of the 16S rRNA gene using forward primer 27F (5′-AGAGTTTGATCCTGGCTCAG-3′) and reverse primer 338R (5′-TGCTGCCTCCCGTAGGAGT-3′). PCR products were purified using a GeneJET™ PCR purification kit (Fermentas, USA) and then sent to an Illumina MiSeq PE300 platform. The obtained sequencing data were stored in the NCBI Sequence Read Archive (accession number of SRP149668). Network-based visualization and principal component analysis (PCA) were also performed to examine the universality and differentiation interrelations of all operational taxonomic units (OTUs) across different recirculation ratios (Chen et al., 2018). Detailed information required for DNA extraction, PCR amplification, 16S rRNA gene Illumina MiSeq sequencing, PCA and network analysis were described in the previous studies (Chen et al., 2019; Lin et al., 2019).

3. Results and discussion

3.1. Response of bioreactor performance to the different recirculation ratios

According to the long-term performances of S^0 transformation and removals of nitrate and acetate, the whole data was divided into three stages including the start-up stage, stable stage and dynamic stage (Fig. 1.). After completion of AGS acclimation, the performance of the three bioreactors increased significantly and tended to be stable during the start-up stage. The S^0 transformation ratio, NO_3^- removal ratio and Ac^- removal ratio in the three bioreactors approached more than 85%, 95% and 93% after 7 d, respectively. During the operation from 8 d to 58 d, no significant difference was observed in the performance of R1, R2 and R3 ($P > 0.1$). S^0 transformation ratio, NO_3^- removal ratio and Ac^- removal ratio were averagely kept at 87.6%, 99.5% and 99.0%, respectively (Fig. 1).

However, after 59 d, the performance of R1, R2 and R3 gradually showed the difference. Specifically, the S^0 transformation ratio of R1 and R3 were reduced to 72.1% and 56.0% within the following 24 days (59 d–82 d), respectively (Fig. 1A). Although the S^0 transformation ratio of R2 exhibited a slight decrease, it could still be maintained at 78.7–88.4% during the dynamic stage. The NO_3^- and Ac^- removal showed a similar trend to S^0 transformation (Fig. 1). The NO_3^- ratio of R2 was still maintained above 95%, while that of R1 and R3 was decreased to 81.6% and 73.5% on 82 d, respectively (Fig. 1B). The Ac^- removal ratio of R3 was reduced to 76.2%, which was 15.9% and 22.2% lower than those in R1 and R2, respectively (Fig. 1C). In general, the performances of the three bioreactors exhibited remarkable differences ($P < 0.01$) during the dynamic stage. It could be preliminarily concluded that the recirculation ratio of 6:1 was more suitable for the long-term operation of the DSR-EGSB bioreactor.

It should be mentioned that N_2O might be produced and accumulated as an intermediate product due to the relatively low N_2O reduction rate during the DSR process (Liu et al., 2016). Recirculation ratios could affect the mass transformation inside granule and subsequently cause the different N_2O accumulation during DSR process by AGS (Sabba et al., 2018; Yang et al., 2016b). It was reasonable that the higher recirculation ratio was more favorable for the mass transformation and biological utilization for N_2O (Yang et al., 2016b). Therefore, it was inferred that higher recirculation ratio reduced N_2O emission.

3.2. Effect of recirculation ratio on S^0 distribution between AGS and effluent

The distribution of total produced S^0 between granule sludge and effluent at the different recirculation ratios was shown in Fig. 2. The average concentration of S^0 in R1 effluent was 61.7 ± 11.0 mg/L, which accounted for 36.2 ± 6.4% of the total produced S^0 (Fig. 2A). When the recirculation ratio was set at 6:1 in R2, the S^0 concentration in effluent was 90.7 ± 7.4 mg/L and the corresponding S^0 recovery ratio was 51.7 ± 4.8%, which were 47.1% and 42.7% higher than those in R1 (Fig. 2B). A higher recirculation ratio of 9:1 in R3 resulted in the enhanced S^0 concentration in effluent of 95.9 ± 13.4 mg/L and S^0 recovery ratio of 56.8 ± 8.1%, respectively (Fig. 2C). These results were consistent with the visual observation of the long-term S^0 accumulation in reactors and transparency change of the effluent (Fig. S2), indicating that the intensified recirculation ratio was beneficial to improve the proportion of S^0 in the effluent. The above result was probably attributed to that part of the biogenic S^0 formed a sparse layer on AGS surface through extracellular macromolecular polymers (e.g., proteins, polysulfides and polythionates) and charge attraction (Chen et al., 2016; Di Capua et al., 2019; Huang et al., 2018), which was not tightly bound with AGS and could be washed away by the intensified hydraulic disturbance caused by the increased recirculation ratio. As shown in Fig. S3, the further separation and concentration of S^0 from the effluent were required to achieve the efficient utilization of biogenic S^0. The reclaimed S^0 could be used as an electron donor for autotrophic denitrification, as a substrate for bioleaching processes and renewable raw material for sulfuric acid production (Chen et al., 2016; Di Capua et al., 2019).

Compared to the 15.5% improvement in S^0 recovery ratio by doubling the recirculation ratio from 3:1 to 6:1, further increasing the recirculation ratio from 6:1 to 9:1 led to a 5.17% slight growth. Since DSR-EGSB reactors were inoculated AGS as the microbial source, another part of the biogenic S^0 would be mixed with microbes, extracellular polymeric substances (EPS) and inorganic matter (Ohmura et al., 1996). These S^0 was difficult to separate from the AGS by increasing recirculation and enhancing physical disturbance. As shown in Fig. 2 and S2, more than 60% of biogenic S^0 remained in R1 and the large S^0 accumulation occurred at the end of R1 operation. Combined with R1 performance (Fig. 1), it was inferred that the decline of mass transfer efficiency caused by excessive S^0 accumulation in AGS might be

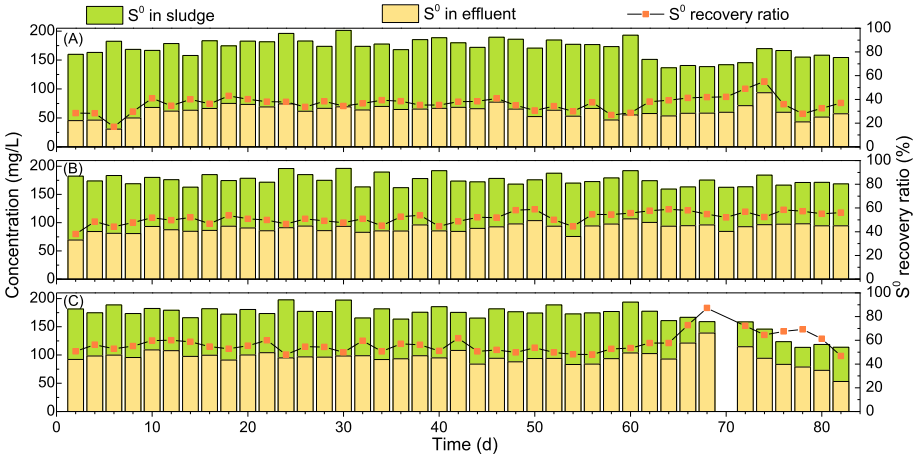

Fig. 2. Distribution of total produced S^0 between sludge and effluent of DSR-EGSB reactors with different recirculation ratios of 3:1 (A), 6:1 (B) and 9:1 (C), respectively.

responsible for the attenuation of R1 performance in the dynamic stage. In addition, the S^0 concentration in R3 effluent fluctuated sharply in dynamic stage (Fig. 2C), which might be attributed to the loss of S^0-containing sludge from the reactor (Fig. S2). Especially, the S^0 concentration in the effluent (147.8 mg/L) was higher than the concentration of total produced S^0 (137.5 mg/L) on 70 d, which led to a false result that the S^0 recovery ratio was greater than 100%. Adequate recirculation ratio could enhance S^0 recovery, but excessive recirculation ratios were likely to cause unstable performance. On the other hand, the higher recirculation ratio demand foreboded higher power consumption. Therefore, the possible "trade-off" between S^0 recovery, reactor stability and operating costs should be considered in the choice of recirculation ratio in the future potential applications.

3.3. Effect of recirculation ratio on AGS characteristics

As shown in Fig. 3, during the long-term operation, R1 showed the highest TSS growth compared to R2 and R3. However, the VSS/TSS ratio in R1 declined from initial 0.50 to 0.33 on 82 d, while that in R2 and R3 could remain at 0.47–0.59 throughout the reactor running (Fig. 3). Similar VSS/TSS ratios ranging from 0.35 to 0.55 were reported during the long-term operation of a sulfur autotrophic denitrification reactor (Yang et al., 2016a). Compared to the high VSS/TSS ratio (around 0.80) of activated sludge, AGS often has low VSS/TSS ratio around 0.50 due to non-volatile materials accumulation (Coma et al., 2012; Yang et al., 2016a). The intensity of hydraulic disturbance in R1 was weaker than that in R2 and R3 due to the lower recirculation ratio (3:1), which caused that S^0 accumulation as inorganic suspended solids in sludge was greater than biomass growth, and led to a decrease in VSS/TSS ratio. It could also be observed in Fig. S2, S^0 accumulation in reactors with different recirculation ratios followed the order of R1 > R2 > R3. As the biogenic S^0 continuously accumulated in AGS, the mass transfer between functional microorganisms and metabolic substrates in the liquid phase was inhibited (Wäsche et al., 2002). Therefore, the decline of R1 performance during the dynamic stage might be attributed to the reduced mass transfer efficiency and weak hydraulic disturbances. The biogenic S^0 particles were covered by multiple long-chain polymers with hydrophilic properties and negative charges, which would disturb the particle aggregation into AGS and further decrease the AGS settling performance (Di Capua et al., 2019; Kleinjan et al., 2003). Therefore, the likelihood of sludge loss from reactors increased at a high recirculation ratio of 9:1 (up-flow velocity of 5 m/h).

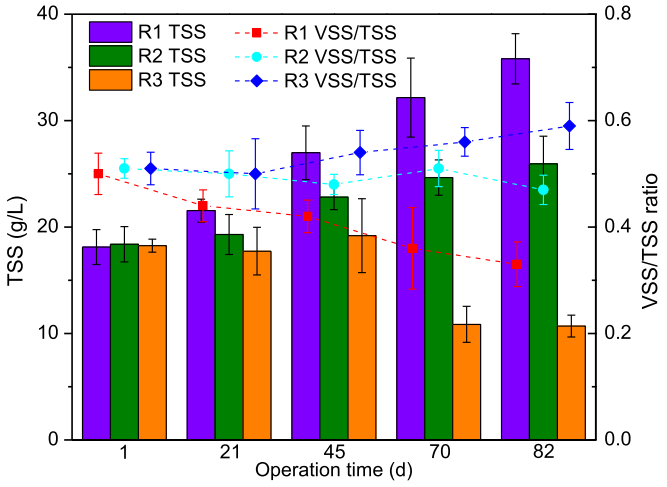

Fig. 3. Variation of TSS concentration and VSS/TSS ratio for DSR-EGSB reactors with different recirculation ratios of 3:1 (A), 6:1 (B) and 9:1 (C), respectively.

TSS concentration in R3 was declined to 10.70 g/L on 82 d, which was 70.1% and 58.8% lower than that in R1 and R2, respectively (Fig. 3). It was inferred that the biomass reduction in R3 might be responsible for the rapid decline in performance at the end of the operation. It was worth noting that sludge loss did not occur in R2 and VSS/TSS ratio maintained relatively stable throughout the operation, which probably attributed to the better operation performance (Figs. 1 and 3). Therefore, the different recirculation ratios regulation significantly altered the biomass components of the sludge, which played important roles in DSR-EGSB performance. In addition, AGS size distribution was chosen as a characteristic parameter to determine the effect of the recirculation ratio on sludge. The AGS size distributions by weight were measured by sieving method at the end of the operation (Fig. 4.). The proportion of AGS with a size of less than 0.3 mm in R3 (9.25%) was significantly lower than that in R1 (15.14%) and R2 (18.08%), indicating that small particles tended to flow out with effluent at high recirculation ratios. However, the proportion of AGS with a size of 0.3–0.6 mm in R3 (accounting for 38.63%) was higher than that in R1 (accounting for 31.76%) and R2 (accounting for 21.15%), respectively. For granule size in the range of 0.3–0.6 mm, there was no obvious difference between the three reactors (corresponding sludge accounting for 29.48%, 27.24% and 30.39%). It was worth to mention that the proportion of AGS larger than 1 mm in diameter in R2 was higher than that in R1 and R3, respectively. Therefore, it could be concluded that recirculation ratio played a crucial role in granule sludge size distributions.

The formation and structure of AGS were closely related to the

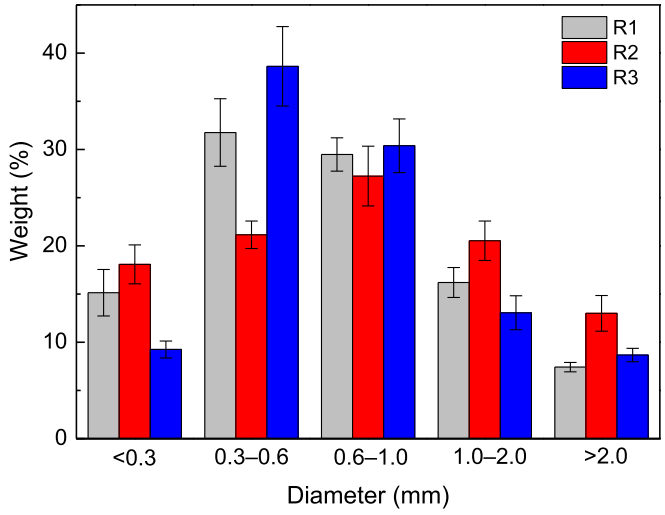

Fig. 4. Granule sludge size distributions by weight (sieving method) at the end of the operation.

hydrodynamic shear force caused by recirculation ratio in EGSB reactors. It was proved that the AGS formation could be regulated by hydrodynamic stress applied to the sludge by increasing up-flow velocity (Liu and Tay, 2002). In DSR-EGSB reactor, the up-flow velocity was controlled by adjusting recirculation ratio. A low liquid up-flow velocity might allow dispersed bacterial growth and would be unfavorable for microbial granulation (Pol et al., 1988), which may be responsible for the weak granulation in R1 with a low recirculation ratio (Fig. 4.). A relatively high liquid up-flow velocity was able to wash out the dispersed bacteria and keep the aggregated bacteria in the reactor (Liu and Tay, 2002). However, the excessive hydrodynamic shear force would cause the AGS fragmentation, consistent with the phenomenon that the proportion of large particles (> 1 mm in diameter) in R3 was lower than that in R2 (Fig. 4). The granule sludge size distribution was consistent with the visual observation of DSR-EGSB reactors at the end of operation (Fig. S2). In addition, EPS, mainly composed of polysaccharides, proteins, lipids, phenols and nucleic acids, played important roles in forming and maintaining AGS (Lim and Kim, 2014). Previous researchers presented that EPS could protect bacteria from the surroundings, such as increasing hydrodynamic turbulence, which was consistent the observation that EPS formation (e.g. protein and polysaccharide) were improved with an increase in up-flow velocity (Wu et al., 2009; Yang et al., 2016a). Hydrodynamic conditions were confirmed to be related to mass transfer of substrates in AGS, and a relatively high hydrodynamic shear force would accelerate the microbial EPS secretion (Liu et al., 2004). In an engineering sense, recirculation ratio could be manipulated as a control parameter to enhance microbial EPS secretion, which was important for maintaining the structure and stability of AGS.

3.4. Effects of recirculation ratio on bacterial diversity and community composition

The 16S rRNA gene-based Illumina MiSeq sequencing generated over 20,000 qualified sequences with an average length of 327 bps for each sample (Table S2). Shannon index showed that R1 held higher biodiversity (1.68) than that of both R2 (1.48) and R3 (1.41) (Table S2). At the phylum level, Proteobacteria were the dominant microbe in R1, R2 and R3 with a relative abundance of 96.1%, 97.6% and 98.0%, respectively (Fig. 5A). At the class level, Betaproteobacteria species were found to be more enriched as the recirculation ratio increased, with relative abundance of 42.7%, 70.8% and 83.6% at a recirculation ratio of 3:1 (R1), 6:1 (R2) and 9:1 (R3), respectively (Fig. 5B). Epsilonproteobacteria species were dominant in R1 with a lower recirculation ratio (accounting for 51.8%), while it was decreased to 25.5% and 12.4% in R2 and R3 with higher recirculation ratios, respectively. At the genus level, three genera in charge of denitrifying sulfur oxidization were predominant at different recirculation ratios, including *Arcobacter* (12.4–51.8%), *Azoarcus* (25.0–66.4%) and *Thauera* (13.7–15.3%) (Fig. 5C).

PCA analysis showed that samples with the different recirculation ratios were located far from each other, which further revealed the differentiation in their functional bacterial community composition (Fig. 6A). Dominating genera such as *Azoarcus* was positively correlated with the higher recirculation ratio condition, whereas *Arcobacter* was positively correlated with the lower recirculation ratio condition. Microbial sharing network analysis showed that the recirculation ratio had an influential role in shaping the topology of the network (Fig. 6B). A total of 74 of 319 OTUs were distributed among all reactors, and exclusive OTUs (90) belonging to R1 with a lower recirculation ratio of 3:1 were more abundant than that in R2 (45) and R3 (32) with a higher recirculation ratio of 6:1 and 9:1, respectively (Fig. 4B), probably attributed to more likely sludge loss at higher recirculation ratios. The shared genera including *Azoarcus*, *Thauera* and *Arcobacter* were typical denitrifying and sulfide-oxidizing functional bacteria and gathered in the center.

The desired influent quality for mixotrophic denitrification achieved the enrichment of autotrophic and heterotrophic denitrifying bacteria. *Arcobacter* sp. was reported to be able to oxidize sulfide autotrophically into filamentous sulfur and simultaneously fix carbon dioxide to organic compounds (Wirsen et al., 2002). Levels of *Arcobacter* decreased from 51.8% to 12.4% and 25.5% as the recirculation ratio further increased from 3:1 to 6:1 and 9:1, respectively (Fig. 5C). *Azoarcus* substituted for *Arcobacter* as the dominant genera, accounting for 55.6% and 66.4% of the total bacterial community at a recirculation ratio of 6:1 and 9:1, respectively. *Azoarcus* was reported as the denitrifying and sulfide-oxidizing bacteria and was able to convert sulfide to S^0 and NO_3^- to N_2 under autotrophic or heterotrophic conditions (Lee and Wong, 2014; Zhang et al., 2018). *Thauera* was one widely known heterotrophic nitrate-reducing bacteria (Etchebehere and Tiedje, 2005), accounting for 14.3%, 13.7% and 15.3% in R1, R2 and R3, respectively. Also, some less abundant bacterial genera such as *Vulcanibacillus* (2.0%) and *Thiobacillus* (1.4%) were found that enriched in R1 with a lower recirculation ratio (Fig. 5C). *Thiobacillus* was a typical autotrophic denitrifier that could oxidize sulfide to S^0 or sulfate with nitrate as the electron acceptor (Pokorna and Zabranska, 2015). *Vulcanibacillus* was also the chemoheterotrophic denitrifying bacteria, which could reduce NO_3^- to NO_2^- rather than N_2 (Apos et al., 2006). These results indicated that facultative and heterotrophic functional bacteria (*Azoarcus* and *Thauera*) were more adapted to higher recirculation ratio than autotrophic functional bacteria (*Arcobacter*, *Thiobacillus* and *Vulcanibacillus*). The distinguishing feature of EGSB reactor was the high up-flow velocity, improving wastewater-granule contact as well as enhancing the outflow of small suspended particles from the reactor. Therefore, the biomass in the suspension was much less than that in the granules. In addition, most of them were derived from the detachment of the granules. Based on the above, we supposed that the contribution of the community mainly relied on the granules. It should also be noticed the biomass in the suspension may still undergo weak DSR activity. Contribution from suspended biomass on the overall performance of the reactor could be further verified by collecting suspensions for bacterial community structure and function analysis. Heterotrophic bacteria secreted more EPS and soluble microbial products (SMP) than autotrophic bacteria, which was conducive to the formation of bacterial aggregates to response to the intensified hydraulic disturbance caused by the increased recirculation ratio (Sheng et al., 2010; Xie et al., 2012).

Based on the above, it was concluded that recirculation ratio regulation could significantly impact the C/N/S removal and S^0 recovery performance of the DSR-EGSB reactor, which was intrinsically

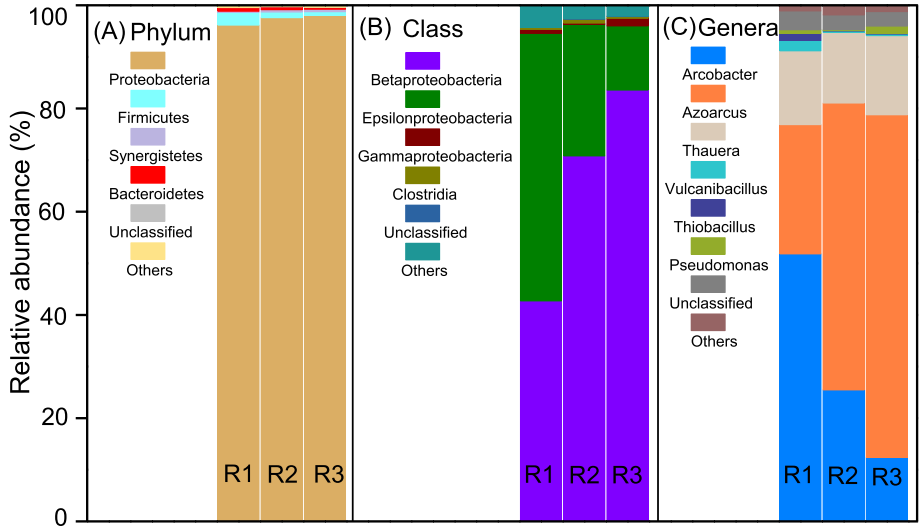

Fig. 5. Bacterial community structures at phylum (A), class (B) and genera (C) levels in DSR-EGSB reactors corresponding to the different recirculation ratio of 3:1 (R1), 6:1 (R2) and 9:1 (R3), respectively.

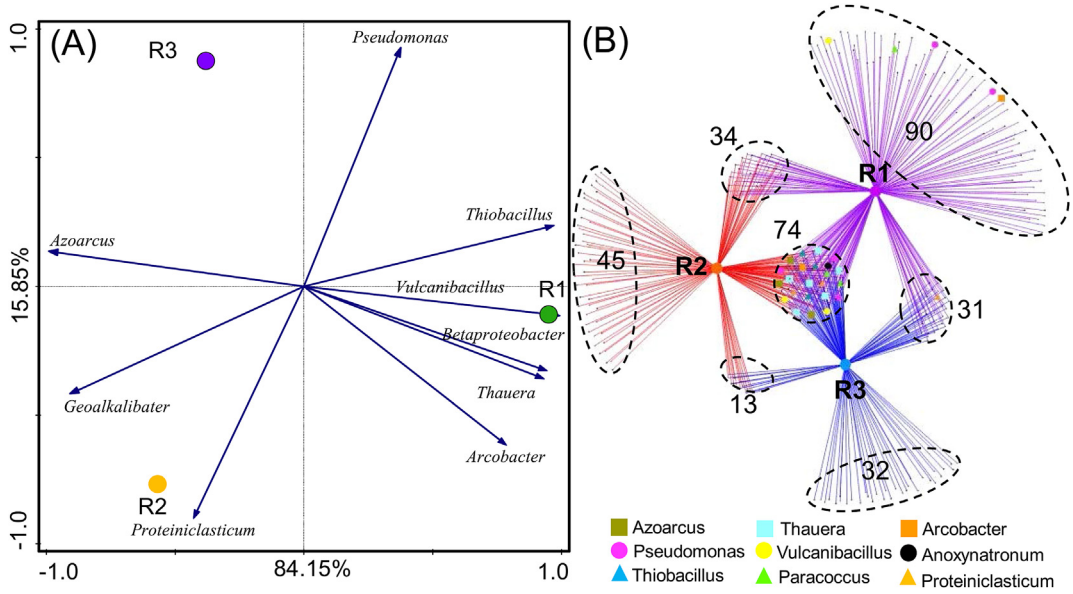

Fig. 6. Principal component analysis (PCA) of the identified operation taxonomic units (OTUs) from DSR-EGSB reactors with a different recirculation ratio of 3:1 (R1), 6:1 (R2) and 9:1 (R3), respectively (A). OTU sharing network of bacterial communities in DSR-EGSB reactors with different recirculation ratios (B).

attributed to the altering of AGS characteristics and microbial community composition in the reactor. In future potential applications, the choice of the recirculation ratio for the DSR-EGSB system should overall considerate the reactor stability, S^0 recovery and operating costs. While the S^0 proportion in the effluent was improved by recirculation regulation, the separation of S^0 from bulk liquids needs further steps. Up to date, flocculation and membrane filtration have been demonstrated as effective approaches for the S^0 separation from the effluent (Chen et al., 2016; Huang et al., 2018). More effort is required to explore more feasible approaches to achieve the efficient separation of S^0 from bulk liquids.

4. Conclusions

Recirculation ratio regulation significantly impacted the DSR-EGSB reactor performance by altering AGS characteristics and microbial community composition. Long-term stable operation of DSR-EGSB system was achieved at an intermediate recirculation ratio of 6:1. Adequate recirculation ratio could enhance S^0 recovery, but excessive recirculation ratios were likely to cause AGS fragmentation and biomass loss. At the low recirculation ratio, S^0 accumulation as inorganic suspended solids in AGS led to a decrease in VSS/TSS ratio and mass transfer efficiency. Biomass components of the AGS played important roles in DSR-EGSB performance, and it could be regulated by applying different recirculation ratios. Although denitrifying and sulfide-oxidizing bacteria were predominant in all conditions, facultative and heterotrophic functional bacteria were more adaptable to higher recirculation ratio than autotrophic ones, which facilitated the formation of bacterial aggregates in response to the intensified hydraulic disturbance caused by the increased recirculation ratio.

Acknowledgements

This research was supported by Heilongjiang Province Natural Science Foundation (C2018035), by Open Project of State Key Laboratory of Urban Water Resource and Environment, Harbin Institute

of Technology (No. ES201806), by Special Financial Grant from China Postdoctoral Science Foundation (2015T80359), and HIT Environment and Ecology Innovation Special Funds (No. HSCJ201621).

Appendix A. Supplementary data

Supplementary data to this article can be found online at https://doi.org/10.1016/j.envres.2019.108905.

References

Apos, Haridon, S., Miroshnichenko, M.L., Kostrikina, N.A., Tindall, B.J., Spring, S., Schumann, P., Stackebrandt, E., Bonch-Osmolovskaya, E.A., Jeanthon, C., 2006. *Vulcanibacillus modesticaldus* gen. nov., sp. nov., a strictly anaerobic, nitrate-reducing bacterium from deep-sea hydrothermal vents. Int. J. Syst. Evol. Microbiol. 56, 1047–1053.

Bhattacharyya, D., Singh, K.S., 2010. Understanding the mixing pattern in an anaerobic expanded granular sludge bed reactor: effect of liquid recirculation. J. Environ. Eng. 136, 576–584.

Chen, C., Ren, N., Wang, A., Yu, Z., Lee, D.-J., 2008. Simultaneous biological removal of sulfur, nitrogen and carbon using EGSB reactor. Appl. Microbiol. Biotechnol. 78, 1057–1063.

Chen, C., Wang, A., Ren, N., Lee, D.-J., Lai, J.-Y., 2009. High-rate denitrifying sulfide removal process in expanded granular sludge bed reactor. Bioresour. Technol. 100, 2316–2319.

Chen, C., Zhang, R.-C., Xu, X.-J., Fang, N., Wang, A.-J., Ren, N.-Q., Lee, D.-J., 2017. Enhanced performance of denitrifying sulfide removal process at high carbon to nitrogen ratios under micro-aerobic condition. Bioresour. Technol. 232, 417–422.

Chen, F., Li, Z.-L., Yang, J.-q., Liang, B., Lin, X.-Q., Nan, J., Wang, A.-J., 2018. Effects of different carbon substrates on performance, microbiome community structure and function for bioelectrochemical-stimulated dechlorination of tetrachloroethylene. Chem. Eng. J. 352, 730–736.

Chen, F., Liang, B., Li, Z.-L., Yang, J.-Q., Huang, C., Lyu, M., Yuan, Y., Nan, J., Wang, A.-J., 2019. Bioelectrochemical assisted dechlorination of tetrachloroethylene and 1,2-dichloroethane by acclimation of anaerobic sludge. Chemosphere 227, 514–521.

Chen, F., Yuan, Y., Chen, C., Zhao, Y., Tan, W., Huang, C., Xu, X., Wang, A., 2016. Investigation of colloidal biogenic sulfur flocculation: optimization using response surface analysis. J. Environ. Sci. 42, 227–235.

Coma, M., Verawaty, M., Pijuan, M., Yuan, Z., Bond, P.L., 2012. Enhancing aerobic granulation for biological nutrient removal from domestic wastewater. Bioresour. Technol. 103, 101–108.

Cui, Y.-X., Guo, G., Biswal, B.K., Chen, G.-H., Wu, D., 2019. Investigation on sulfide-oxidizing autotrophic denitrification in moving-bed biofilm reactors: an innovative approach and mechanism for the process start-up. Int. Biodeterior. Biodegrad. 140, 90–98.

De Graaff, M., Klok, J.B.M., Bijmans, M.F.M., Muyzer, G., Janssen, A.J.H., 2012. Application of a 2-step process for the biological treatment of sulfidic spent caustics. Water Res. 46, 723–730.

Di Capua, F., Pirozzi, F., Lens, P.N.L., Esposito, G., 2019. Electron donors for autotrophic denitrification. Chem. Eng. J. 362, 922–937.

Etchebehere, C., Tiedje, J., 2005. Presence of two different active nirS nitrite reductase genes in a denitrifying *Thauera* sp. from a high-nitrate-removal-rate reactor. Appl. Environ. Microbiol. 71, 5642–5645.

Faria, C.V., Souza, D.F., Pontes, T.M., Amaral, M.C.S., Fonseca, F.V., 2019. Strategies of anaerobic sludge granulation in an EGSB reactor. J. Environ. Manag. 244, 69–76.

Hao, T.-w., Xiang, P.-y., Mackey, H.R., Chi, K., Lu, H., Chui, H.-k., van Loosdrecht, M.C.M., Chen, G.-H., 2014. A review of biological sulfate conversions in wastewater treatment. Water Res. 65, 1–21.

He, Z.-W., Tang, C.-C., Liu, W.-Z., Ren, Y.-X., Guo, Z.-C., Zhou, A.-J., Wang, L., Yang, C.-X., Wang, A.-J., 2019. Enhanced short-chain fatty acids production from waste activated sludge with alkaline followed by potassium ferrate treatment. Bioresour. Technol. 289, 121642.

Huang, C., Li, Z.-l., Chen, F., Liu, Q., Zhao, Y.-k., Zhou, J.-z., Wang, A.-j., 2015a. Microbial community structure and function in response to the shift of sulfide/nitrate loading ratio during the denitrifying sulfide removal process. Bioresour. Technol. 197, 227–234.

Huang, C., Li, Z.L., Chen, F., Liu, Q., Zhao, Y.K., Gao, L.F., Chen, C., Zhou, J.Z., Wang, A.J., 2016. Efficient regulation of elemental sulfur recovery through optimizing working height of upflow anaerobic sludge blanket reactor during denitrifying sulfide removal process. Bioresour. Technol. 200, 1019–1023.

Huang, C., Liu, Q., Chen, C., Chen, F., Zhao, Y.-K., Gao, L.-F., Liu, W.-Z., Zhou, J.-Z., Li, Z.-L., Wang, A.-J., 2017. Elemental sulfur recovery and spatial distribution of functional bacteria and expressed genes under different carbon/nitrate/sulfide loadings in upflow anaerobic sludge blanket reactors. J. Hazard Mater. 324, 48–53.

Huang, C., Liu, W.-Z., Li, Z.-L., Zhang, S.-M., Chen, F., Yu, H.-R., Shao, S.-L., Nan, J., Wang, A.-J., 2018. High recycling efficiency and elemental sulfur purity achieved in a biofilm formed membrane filtration reactor. Water Res. 130, 1–12.

Huang, C., Zhao, Y., Li, Z., Yuan, Y., Chen, C., Tan, W., Gao, S., Gao, L., Zhou, J., Wang, A., 2015b. Enhanced elementary sulfur recovery with sequential sulfate-reducing, denitrifying sulfide-oxidizing processes in a cylindrical-type anaerobic baffled reactor. Bioresour. Technol. 192, 478–485.

Huang, H., Ekama, G.A., Biswal, B.K., Dai, J., Jiang, F., Chen, G.-H., Wu, D., 2019. A new sulfidogenic oxic-settling anaerobic (SOSA) process: the effects of sulfur-cycle bioaugmentation on the operational performance, sludge properties and microbial communities. Water Res. 162, 30–42.

Ji, G.D., Sun, T.H., Ni, J.R., Tong, J.J., 2009. Anaerobic baffled reactor (ABR) for treating heavy oil produced water with high concentrations of salt and poor nutrient. Bioresour. Technol. 100, 1108–1114.

Jin, R.-C., Yang, G.-F., Zhang, Q.-Q., Ma, C., Yu, J.-J., Xing, B.-S., 2013. The effect of sulfide inhibition on the ANAMMOX process. Water Res. 47, 1459–1469.

Kleinjan, W.E., de Keizer, A., Janssen, A.J.H., 2003. Biologically produced sulfur. In: Steudel, R. (Ed.), Elemental Sulfur and Sulfur-Rich Compounds I. Springer, Berlin, Heidelberg, pp. 167–188.

Lee, D.-J., Wong, B.-T., 2014. Denitrifying sulfide removal and nitrososulfide complex: *Azoarcus* sp. NSC3 and *Pseudomonas* sp. CRS1 mix. Bioresour. Technol. 166, 616–619.

Lim, S.J., Kim, T.-H., 2014. Applicability and trends of anaerobic granular sludge treatment processes. Biomass Bioenergy 60, 189–202.

Lin, X.-Q., Li, Z.-L., Liang, B., Zhai, H.-L., Cai, W.-W., Nan, J., Wang, A.-J., 2019. Accelerated microbial reductive dechlorination of 2, 4, 6-trichlorophenol by weak electrical stimulation. Water Res. 162, 236–245.

Liu, Y.-Q., Liu, Y., Tay, J.-H., 2004. The effects of extracellular polymeric substances on the formation and stability of biogranules. Appl. Microbiol. Biotechnol. 65, 143–148.

Liu, Y., Peng, L., Ngo, H.H., Guo, W., Wang, D., Pan, Y., Sun, J., Ni, B.-J., 2016. Evaluation of nitrous oxide emission from sulfide-and sulfur-based autotrophic denitrification processes. Environ. Sci. Technol. 50, 9407–9415.

Liu, Y., Tay, J.-H., 2002. The essential role of hydrodynamic shear force in the formation of biofilm and granular sludge. Water Res. 36, 1653–1665.

Ohmura, N., Tsugita, K., Koizumi, J.I., Saika, H., 1996. Sulfur-binding protein of flagella of *Thiobacillus ferrooxidans*. J. Bacteriol. 178, 5776.

Pokorna, D., Zabranska, J., 2015. Sulfur-oxidizing bacteria in environmental technology. Biotechnol. Adv. 33, 1246–1259.

Pol, L.H., Heijnekamp, K., Lettinga, G., 1988. The Selection Pressure as a Driving Force behind the Granulation of Anaerobic Sludge. Granular Anaerobic Sludge: Microbiology and Technology. Kluwer Wageningen, pp. 153–161.

Sabba, F., Terada, A., Wells, G., Smets, B.F., Nerenberg, R., 2018. Nitrous oxide emissions from biofilm processes for wastewater treatment. Appl. Microbiol. Biotechnol. 102, 9815–9829.

Sheng, G.-P., Yu, H.-Q., Li, X.-Y., 2010. Extracellular polymeric substances (EPS) of microbial aggregates in biological wastewater treatment systems: a review. Biotechnol. Adv. 28, 882–894.

Show, K.-Y., Lee, D.-J., Pan, X., 2013. Simultaneous biological removal of nitrogen–sulfur–carbon: recent advances and challenges. Biotechnol. Adv. 31, 409–420.

Wäsche, S., Horn, H., Hempel, D.C., 2002. Influence of growth conditions on biofilm development and mass transfer at the bulk/biofilm interface. Water Res. 36, 4775–4784.

Wang, A., Liu, C., Han, H., Ren, N., Lee, D.-J., 2009. Modeling denitrifying sulfide removal process using artificial neural networks. J. Hazard Mater. 168, 1274–1279.

Wirsen, C.O., Sievert, S.M., Cavanaugh, C.M., Molyneaux, S.J., Ahmad, A., Taylor, L.T., DeLong, E.F., Taylor, C.D., 2002. Characterization of an autotrophic sulfide-oxidizing marine *Arcobacter* sp. that produces filamentous sulfur. Appl. Environ. Microbiol. 68, 316–325.

Wu, D., Ekama, G.A., Chui, H.-K., Wang, B., Cui, Y.-X., Hao, T.-W., van Loosdrecht, M.C.M., Chen, G.-H., 2016. Large-scale demonstration of the sulfate reduction autotrophic denitrification nitrification integrated (SANI®) process in saline sewage treatment. Water Res. 100, 496–507.

Wu, J., Zhou, H.-m., Li, H.-z., Zhang, P.-c., Jiang, J., 2009. Impacts of hydrodynamic shear force on nucleation of flocculent sludge in anaerobic reactor. Water Res. 43, 3029–3036.

Xie, W.-M., Ni, B.-J., Seviour, T., Sheng, G.-P., Yu, H.-Q., 2012. Characterization of autotrophic and heterotrophic soluble microbial product (SMP) fractions from activated sludge. Water Res. 46, 6210–6217.

Yang, W., Lu, H., Khanal, S.K., Zhao, Q., Meng, L., Chen, G.-H., 2016a. Granulation of sulfur-oxidizing bacteria for autotrophic denitrification. Water Res. 104, 507–519.

Yang, W., Zhao, Q., Lu, H., Ding, Z., Meng, L., Chen, G.-H., 2016b. Sulfide-driven autotrophic denitrification significantly reduces N_2O emissions. Water Res. 90, 176–184.

Yuan, Y., Bian, A., Chen, F., Xu, X., Huang, C., Chen, C., Liu, W., Cheng, H., Chen, T., Ding, C., Li, Z., Wang, A., 2019. Continuous sulfur biotransformation in an anaerobic-anoxic sequential batch reactor involving sulfate reduction and denitrifying sulfide oxidization. Chemosphere 234, 568–578.

Zhang, R.-C., Xu, X.-J., Chen, C., Xing, D.-F., Shao, B., Liu, W.-Z., Wang, A.-J., Lee, D.-J., Ren, N.-Q., 2018. Interactions of functional bacteria and their contributions to the performance in integrated autotrophic and heterotrophic denitrification. Water Res. 143, 355–366.

Zheng, M.X., Wang, K.J., Zuo, J.E., Yan, Z., Fang, H., Yu, J.W., 2012. Flow pattern analysis of a full-scale expanded granular sludge bed-type reactor under different organic loading rates. Bioresour. Technol. 107, 33–40.